In Vento M., Percannella G. (eds): Computer Analysis of Images and Patterns.
Lecture Notes in Computer Science, Vol. 11678, 102-112, Springer, Cham, 2019.
The final publication is available at link.springer.com

Hough Based Evolutions for Enhancing Structures in 3D Electron Microscopy

Kireeti Bodduna[1,2,3], Joachim Weickert[1], and Achilleas S. Frangakis[2]

[1] Mathematical Image Analysis Group,
Faculty of Mathematics and Computer Science,
Saarland University, 66041 Saarbrücken, Germany.
{bodduna, weickert}@mia.uni-saarland.de
[2] Electron Microscopy Group, Institute of Biophysics,
Johann Wolfgang Goethe University Frankfurt,
60438 Frankfurt am Main, Germany.
{bodduna, achilleas.frangakis}@biophysik.org
[3] Saarbrücken Graduate School of Computer Science,
Saarland University, 66041 Saarbrücken, Germany.

Abstract. Connecting interrupted line-like structures is a frequent problem in image processing. Here we focus on the specific needs that occur in 3D biophysical data analysis in electron microscopy (EM). We introduce a powerful framework for connecting line-like structures in 3D data sets by combining a specific semilocal Hough transform with a directional evolution equation. The Hough transform allows to find the principal orientations of the local structures in a robust way, and the evolution equation is designed as a partial differential equation that smoothes along these principal orientations. We evaluate the performance of our method for enhancing structures in both synthetic and real-world EM data. In contrast to traditional structure tensor based methods such as coherence-enhancing diffusion, our method can handle the missing wedge problem in EM, also known as limited angle tomography problem. A modified version of our approach is also able to tackle the discontinuities created due to the contrast transfer function correction of EM images.

Keywords: Structure enhancement, electron microscopy, Hough transform, partial differential equations, missing wedge problem.

1 Introduction

Enhancing oriented structures is a classical problem in image processing. Grading the quality of fabrics and wood, fingerprint analysis, and processing cellular structures from electron microscopes are specific areas where enhancing oriented

structures is required. On a broader scale, this application is encountered in fluid dynamics, meteorology, forensic studies, computer vision, biomedical and biophysical image analysis.

In 2D, analysing and processing oriented structures has a long tradition, and the structure tensor [6] and its equivalent concepts plays a prominent role in this context. While early work by Kass and Witkin [12] and Rao and Schunck [16] apply it as a pure analysis tool, Weickert et al. [20, 21] use it to steer a so-called coherence-enhancing anisotropic diffusion (CED) process. This has triggered several follow up works that employ diffusion based ideas to enhance oriented structures [9, 17, 19]. Mühlich et al. [14] have studied the presence of multiple orientations in a local neighbourhood. Stochastic models [22] have also been used for analysis of contour shapes in images. More recently, template matching based on orientation scores [3] has been proposed for detecting combined orientation and blob patterns.

In 3D, the first technique for coherence enhancement was proposed by Weickert et al. [21]. Related works to this anisotropic diffusion technique in 3D include papers by Krissian et al. [13] and by Payot et al. [15] for medical imaging applications. Also in our days, methods based on partial differential equations continue to be important for enhancing 3D data sets that are difficult and expensive to acquire, such that deep learning approaches are less suited. However, in order to achieve optimal quality, these methods should be well adapted to the imaging process.

Our Goals. In our work, the main goal is to design a filter that extends the application of oriented structure enhancement in 3D to the specific needs in Electron Microscopy (EM). One challenge in designing filters for EM data is the limited angle tomography problem, also known as missing wedge problem [7, 8]. It arises from the geometric design of data acquisition using the electron microscope. One cannot acquire data from all orientations of the sample, which leads to presence of the missing wedge in the Fourier space. When one reconstructs the 3D data in the Cartesian space from individual projections, the data is blurred/smeared in the directions where the missing wedge exists. Figure 1 shows the directions in which the data is blurred at every pixel in the Cartesian space. Here we depict a particular xz plane. The two triangles represent the directions where the data is smeared at every pixel. This region extends throughout the y direction. Due to the smearing effect of the data, classical formulas based on gradient calculations cannot be considered for processing this reconstructed data in order to enhance the image structures. Another challenge in EM is created by discontinuities in the image structures due to the contrast transfer function (CTF) correction of EM data. We will see that the direct and modified approaches of the Hough based evolution (HE) method introduced by us in this work is effective in dealing with both problems.

Paper Structure. The organisation of our paper is as follows: In Section 2 we introduce the HE method. We also mention the specific changes that have to be made to the classical ideas used for structure enhancement, in order to adapt

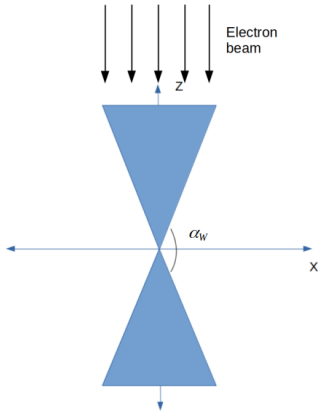

Fig. 1: Directions where the data is smeared at every pixel in Cartesian space due the presence of the missing wedge.

them to electron microscopy data. In Section 3, we compare the performance of the HE method with the popular CED approach on synthetic and EM data. We also discuss how the ideas used in the modelling of the HE algorithm lead to the desired enhancement of oriented structures in the images. In Section 4, we conclude with a summary and give an outlook to future work.

2 Hough Based Evolution

2.1 A General Directional Data Evolution

Let $\Omega \subset \mathbb{R}^3$ denote a cuboid and consider some 3D data set $f : \Omega \to \mathbb{R}$. We can obtain a family $\{u(.,t) \,|\, t \geq 0\}$ of smoothed versions of f by regarding f as initial value of a 3D directional image evolution that satisfies the following partial differential equation:

$$\partial_t u = \partial_{\eta\eta} u = \boldsymbol{\eta}^\top \mathrm{Hess}(u)\, \boldsymbol{\eta} \tag{1}$$

with reflecting boundary conditions. Here $\mathrm{Hess}(u)$ denotes the spatial Hessian of u. The smoothing direction $\boldsymbol{\eta}$ is space-variant and is characterised by its angles $\theta(\boldsymbol{x})$ and $\phi(\boldsymbol{x})$ in the spherical coordinate system:

$$\boldsymbol{\eta} = \boldsymbol{\eta}(\boldsymbol{x}) = \begin{pmatrix} \sin(\theta(\boldsymbol{x}))\cos(\phi(\boldsymbol{x})) \\ \sin(\theta(\boldsymbol{x}))\sin(\phi(\boldsymbol{x})) \\ \cos(\theta(\boldsymbol{x})) \end{pmatrix}. \tag{2}$$

Equations of type (1) have a long tradition, in particular in the 2D setting. For instance, for 2D mean curvature motion [1], one chooses $\boldsymbol{\eta}(\boldsymbol{x},t) \perp \boldsymbol{\nabla} u(\boldsymbol{x},t)$.

Pseudo Code: Hough based Evolution

Input: Original discrete data set $\boldsymbol{f}$ and the following parameters:
ρ_1 - radius of the sphere shaped neighbourhood,
ρ_2 - half of the length of the line segments,
T - threshold for the Hough transform,
τ - time step size of the explicit scheme,
$k_{\max}$ - total number of iterations.

Modified Hough Algorithm for Computing $\boldsymbol{\eta}(\boldsymbol{x})$:

1. Select a ball B of radius ρ_1 around each pixel of $\boldsymbol{f}$.
2. Line segments of half length ρ_2 centered at every pixel within B are considered by discretising the angles θ and ϕ.
3. The θ and ϕ values of the line segment which has the largest percentage of pixels with grey values $> T$ represent the local dominant direction $\boldsymbol{\eta}$.
   To tackle the missing wedge, only line segments within the angle α_W from Figure 1 are considered in the voting process.

Main Algorithm:

1. Initialisation: $\boldsymbol{u}^0 = \boldsymbol{f}$
2. **For** $k = 0, 1, 2, ..., k_{\max} - 1$:
   $\boldsymbol{u}^{k+1} = \boldsymbol{u}^k + \tau \cdot \boldsymbol{\eta}^\top \mathrm{Hess}(\boldsymbol{u}^k)\ \boldsymbol{\eta}$,
   where $\mathrm{Hess}(\boldsymbol{u}^k)$ is approximated with central finite differences.

Output: Image with enhanced structures $\boldsymbol{u}^{k_{\max}}$.

Obviously such a choice – which smoothes along isophotes – cannot close interrupted structures. To this end, one needs more advanced local structure descriptors than the gradient, e.g. the Gabor transform based methods that are used in the evolution equation of Carmona and Zhong [4]. The Carmona–Zhong approach, however, is designed for processing 2D images and has not been adapted to tackle 3D EM data. We prefer another local structure descriptor that is etter suited for our specific needs. It is based on a semilocal Hough transform and shall be discussed next.

2.2 Choosing the Smoothing Direction with a Hough Transform

The novelty of our work is that we choose the smoothing direction $\boldsymbol{\eta}(\boldsymbol{x})$ mentioned above using a semilocal Hough transform [2, 5, 11] on the original data f. To be more precise, we compute the Hough transform to find the direction $\boldsymbol{\eta}(\boldsymbol{x})$ corresponding to the line segment in a local neighbourhood, which represents the orientation along which the image structure to be enhanced is present. It has to be mentioned that the Hough transform is very robust in detecting the local dominant direction because a small relative majority in the voting process suffices for obtaining the dominant direction. In this sense, for noise of isotropic

nature, the Hough based image evolution is more robust when compared to structure tensor based methods such as CED. Moreover, as we will see in the upcoming section, our modified Hough based selection of dominant directions is able to tackle the missing wedge in EM. The above mentioned pseudo-code explains the complete algorithm and its parameters in detail.

Note that we compute the Hough transform only for the initial data set f, not for its evolution $u(.,t)$. This saves computational time and leads to a linear method. We have not noticed qualitative differences compared to a nonlinear variant where we adapt the dominant direction to the evolving image $u(.,t)$.

2.3 Modification of Classical Ideas for Adapting to EM Data

Let us now discuss the exact modifications we have made to classical concepts in order to adapt them better to the scenario of limited angle tomography.

Restricting the Search Space of Dominant Directions. It was already explained in Section 1 that the missing wedge problems arises due to the design of the data acquistion process: The specimen whose images are acquired cannot be tilted above a certain angle (generally 60^o). Thus, we do not have projections from all the angles. This leads to missing information while reconstructing the 3D data from the available projections, which creates a smearing effect of the reconstructed data in the directions where the data cannot be collected. In order to tackle this, the modified Hough algorithm mentioned above just considers the line segments which are outside the wedge represented in Figure 1, in the voting process. In other words, since our aim is to enhance the structures in the directions where we do not encounter the smearing effect, the search space of Hough directions is restricted by choosing $\alpha_W = 30^0$ (Figure 1). This value is chosen such that the search space is smaller than the entire space representing the directions where the data is not smeared.

Avoiding the Usage of Gradients. Due to the smearing effect of the EM data, classical formulas for gradient calculation can no longer be used for processing. Generally, gradients calculated on a Gaussian-smoothed image (with standard deviation σ) are used for making the decision in the voting process of the Hough transform. We instead use the grey values for making this decision as mentioned in the modified Hough algorithm. If dark structures are to be enhanced, we choose as Hough direction in 3D the one that contains the largest percentage of pixels with greyscale value below a certain threshold. For enhancing bright structures, we consider pixels above the threshold. Most of the previously designed filters mentioned in Section 1 are based on the structure tensor [6]. The structure tensor averages directional information over a local neighbourhood using gradient formulation. Thus, as we will see in the upcoming section, both gradient based Hough algorithm and CED (which is built upon the structure tensor) are not successful in enhancing the structures. On the other hand, we will also see that the usage of the grey value based Hough algorithm in the directional image evolution produces the desired results.

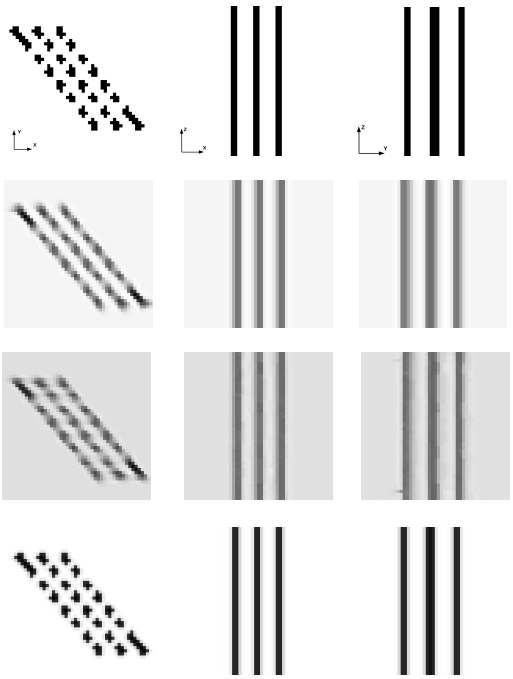

Fig. 2: Performance of the different approaches for a synthetic data set of size $49 \times 49 \times 49$. **Left to Right:** xy, xz, and yz slices. **(a) First Row:** Original data. **(b) Second Row:** Grey value based HE ($\rho_1 = 3$, $\rho_2 = 21$, $T = 10$, $\tau = 0.1$, $k_{\max} = 10$). **(c) Third Row:** Gradient based HE ($\rho_1 = 3$, $\rho_2 = 21$, $T = 5$, $\sigma = 0.5$, $\tau = 0.1$, $k_{\max} = 10$). **(d) Fourth Row:** CED ($\lambda = 1.0$, $\sigma = 0.5$, $\rho = 5.0$, $\alpha = 0.001$, $\tau = 0.1$, $k_{\max} = 1000$).

2.4 Numerical Algorithm

For discretising the 3D evolution equation (1), we use a straighforward explicit scheme as mentioned in the main algorithm of the pseudo-code. We use central derivative approximations to calculate the spatial derivatives in the Hessian. For a spatial grid size of 1, we observe experimentally L^2-stability if the time step size τ satisfies $\tau < \frac{1}{6}$. This stability bound is identical to the one for an explicit scheme for 3D homogeneous diffusion filtering. A more detailed theoretical study of the Hough based image evolution behaviour will be a topic for future research.

3 Results and Discussion

3.1 Synthetic Data

The Shepp–Logan phantom data set [10, 18] is a popular synthetic data set used for testing 3D reconstruction algorithms. However, it is not suited for testing the

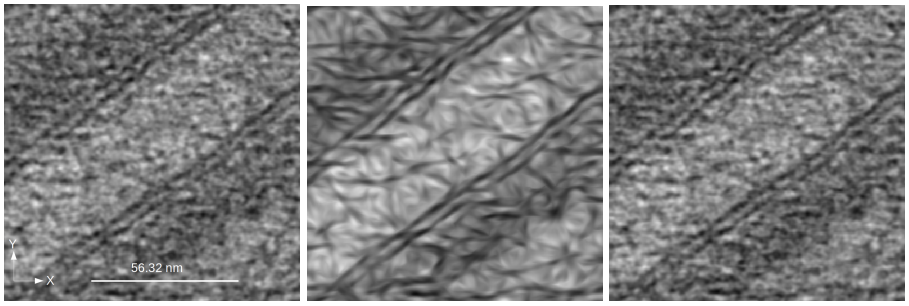

(a) xy slice (b) HE (c) CED

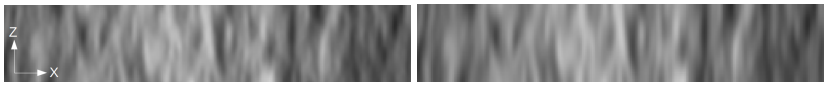

(d) xz slice (e) CED output xz slice

Fig. 3: Cellular regions of rat liver enhanced using 3D HE. In Figure 3(b) we can see the enhanced double walled cell membranes of neighbouring cells. We can also see the desmosomes (structures made of proteins) in directions perpendicular to the cell membrane. HE parameters: $\rho_1 = 3$, $\rho_2 = 21$, $T = 200$, $\tau = 0.1$, $k_{\max} = 50$. CED parameters: $\lambda = 1.0$, $\sigma = 0.5$, $\rho = 5.0$, $\alpha = 0.001$, $\tau = 0.1$, $k_{\max} = 100$. Data set size: $256 \times 256 \times 50$.

capability of enhancing line-like structures in the presence of a missing wedge. A synthetic image for testing this particular capability of methods is simply missing in the image processing community. Thus, we have created a 3D image which mimics the effect of the missing wedge and also has discontinuous structures that need to be connected while enhancing them. Figure 2(a) shows different slices of the 3D data set we have created. We can clearly see the disconnected structures in the xy slice and the elongated/smeared structures in the other slices. This mimics the effect of the missing wedge. Figure 2(b) depicts the results of our grey value based HE method. It is able to connect the disconnected structures. We observe that this approach outperforms both the gradient based HE method and CED whose results are presented in Figures 2(c) and 2(d), respectively.

3.2 Real World Data

Figure 3(a),(d) shows a reconstructed 3D cellular region acquired from an electron microscope. One can see that the data in the z direction is smeared and resembles the above mentioned synthetic data set. Figure 3(b) displays the resulting enhanced cell structures using the HE algorithm. This image allows better visualisations than the original image in Figure 3(a). The enhanced image (Figure 3(b)) contains two double walled cell membranes of neighbouring cells. The structures arising in directions perpendicular to the cell membrane are the desmosome networks which are made of proteins. These networks bind neigh-

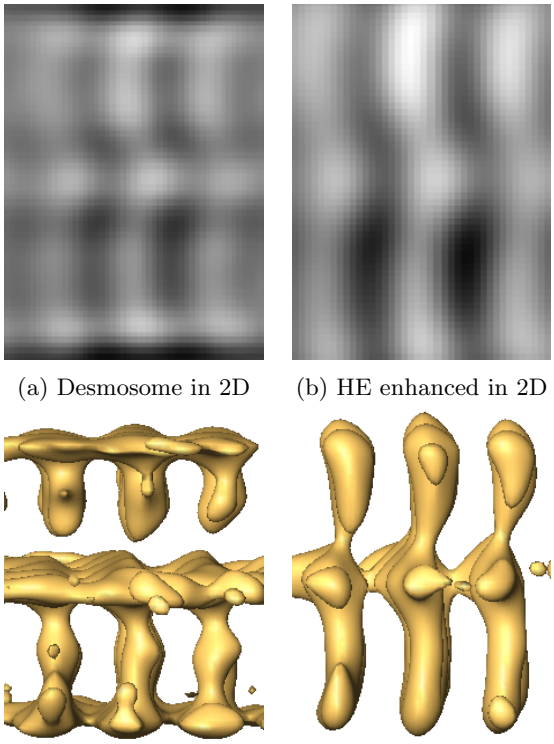

(a) Desmosome in 2D (b) HE enhanced in 2D

(c) Desmosome in 3D (d) HE enhanced in 3D

Fig. 4: Connecting disconnected desmosome structures. Visualisation threshold for both structures is 140. The length of each vertical desmosome is around 28 nm. Full data set size: $128 \times 128 \times 128$. Parmeters used: $\tau = 0.025,\ k_{\max} = 300$.

bouring cells together. The structures are more evident in the enhanced image than the original image (Figure 3(a)). Also, since the original image has more signal in the intra-cellular region than the extra-cellular region, the enhanced image also has clear desmosome networks in the intra-cellular region. Figure 3(c) depicts the result using CED with a straightforward explicit scheme. This structure tensor based enhancement method fails to enhance the structures in the presence of the missing wedge, as was explained in Section 2.3. Figure 3(e) shows the xz slice after applying CED. In the presence of a missing wedge, this method would always smooth in the z-direction as is visible in the image. This is because CED always detects the coherent structures in the z-direction. Consequently, we do not get the desired structure enhancement in the xy slices; see Figure 3(c). In the grey value based HE method, on the other hand, this is avoided by restricting the search space of angles and using grey value based detection of dominant orientations.

Another application of the HE is presented in Figure 4. The vertical structures in white in Figure 4(a) are discontinuous desmosomes. We infer that the presence of discontinuities in the horizontal direction is due the CTF correction of the data after acquisition. We see the desmosome structures in the extra-cellular regions clearly when compared to the images in the previous experiment. This is because several similar structures were averaged to get this final image. Due to this averaging, the missing wedge effect is minimised. Also, we just want to enhance the structures only in the direction perpendicular to the discontinuities. Hence, we need not perform the Hough transform. Smoothing in this required direction is governed by setting $\theta = 0^{\circ}$. The result after removing the discontinuities using HE is displayed in Figure 4(b). The graphical renderings of these structures are depicted in Figure 4. The vertical structures are nicely connected.

It has to be mentioned that the cell structure data sets underwent an affine rescaling to [0, 255] before the algorithms were applied. This facilitates the reproducibility of results while selecting the threshold parameter. It does not have any other effect on the model itself.

3.3 Parameter Selection

There are five parameters which need to be selected, out of which mainly two of them are critical and need to be adapted to the specific data set.

The radius of the sphere ρ_1, half of the length of the line segment ρ_2 and the threshold T for voting process in the Hough transform are the model parameters. The time step size τ and the number of iterations $k_{\max}$ are numerical parameters to reach a desired stopping time.

As already mentioned, τ has to obey a stability criterion caused by the explicit scheme. Fixing τ implies that the stopping time is proportional to $k_{\max}$. We obtain smoother data for a larger number of iterations. Also, if the gaps to be closed are large, we need to increase the number of iterations until the structures get connected.

We suggest $\rho_1 = 3$ for the radius of the sphere shaped neighbourhood. This allows for searching the dominant orientation in a small neighbourhood instead of just around a specific pixel.

The selection of the parameters ρ_2 and T is important. They must be adapted to the data set. The parameter ρ_2, which specifies the length of the line segment, must be greater than the length of the discontinuites in order to detect and remove them. The threshold parameter T for the Hough transform voting process must be selected according to the greyscale range at which the structures are present in the image.

The spherical polar coordinate angles θ and ϕ are sampled 18 times each in their respective ranges.

Performing Gaussian smoothing and specifying the Gaussian standard deviation σ is only necessary for a gradient based Hough transform, due to the ill-posedness of differentiation. It is not required for our grey value based variant.

3.4 Computational Time

All the experiments in this work have been performed with ANSI C and CUDA on an Nvidia Quadro P5000 device. The computational time for the synthetic data experiment with grey value based HE method is 3.45 seconds. The time consumed for the real world data experiments is 84.6 seconds and 10 seconds, respectively.

4 Conclusions and Outlook

We have introduced a method that combines a semilocal Hough transform with a directional image evolution. This approach is designed to enhance oriented structures in 3D data sets from electron microscopy. Our variant of the Hough transform is robust with respect to the unwanted effects produced by the missing wedge effect in EM data. This helps to enhance structures in the data that are present in the directions where no smearing due to the missing projections occurs. Other methods which are based on derivative information, such as CED and gradient based HE, fail to overcome this problem. Additionally, our approach is also able to deal with the discontinuities that can occur in EM data due to the CTF correction.
In our future work we plan to also study applications beyond electron microscopy where the data acquisition is performed in a similar manner.

Acknowledgements. J.W. has received funding from the European Research Council (ERC) under the European Union's Horizon 2020 research and innovation programme (grant agreement no. 741215, ERC Advanced Grant INCOVID).

References

1. Alvarez, L., Lions, P.L., Morel, J.M.: Image selective smoothing and edge detection by nonlinear diffusion. II. SIAM Journal on Numerical Analysis **29**(3), 845–866 (Mar 1991)
2. Ballard, D.H.: Generalizing the Hough transform to detect arbitrary shapes. Pattern Recognition **13.2**(111-122) (1981)
3. Bekkers, E.J., Loog, M., ter Haar Romeny, B.M., Duits, R.: Template matching via densities on the roto-translation group. IEEE Transactions on Pattern Analysis and Machine Intelligence **40**(2), 452–466 (Feb 2018)
4. Carmona, R., Zhong, S.: Adaptive smoothing respecting feature directions. IEEE Transactions on Image Processing **7**(3), 353–358 (Mar 1998)
5. Duda, R., Hart, P.E.: Use of the Hough transformation to detect lines and curves in pictures. Communications of the ACM **15**(1), 11–15 (Jan 1972)
6. Förstner, W., Gülch, E.: A fast operator for detection and precise location of distinct points, corners and centres of circular features. In: Proc. ISPRS Intercommission Conference on Fast Processing of Photogrammetric Data. pp. 281–305. Interlaken, Switzerland (Jun 1987)

7. Frank, J.: Three-dimensional Electron Microscopy of Macromolecular Assemblies: Visualization of Biological Molecules in their Native State. Oxford University Press, Oxford (2006)
8. Frank, J.: Electron Tomography: Three-dimensional Imaging with the Transmission Electron Microscope. Springer, New York (2013)
9. Franken, E., Duits, R., ter Haar Romeny, B.: Nonlinear diffusion on the 2D Euclidean motion group. In: Sgallari, F., Murli, F., Paragios, N. (eds.) Scale Space and Variational Methods in Computer Vision, Lecture Notes in Computer Science, vol. 4485, pp. 461–472. Springer, Berlin (2007)
10. Gach, H.M., Tanase, C., Boada, F.: 2d & 3d Shepp-Logan phantom standards for MRI. In: Proc. 2008 IEEE International Conference on Systems Engineering. pp. 521–526. Las Vegas, NV, USA (Aug 2008)
11. Hough, P.: Methods and means for recognising complex patterns. U.S. Patent No. 3,069,654 (Dec 1962)
12. Kass, M., Witkin, A.: Analyzing oriented patterns. Computer Vision, Graphics and Image Processing **37**, 362–385 (Mar 1987)
13. Krissian, K., Malandain, G., Ayache, N.: Directional anisotropic diffusion applied to segmentation of vessels in 3D images. In: ter Haar Romeny, B., Florack, L., Koenderink, J., Viergever, M. (eds.) Scale-Space Theory in Computer Vision, Lecture Notes in Computer Science, vol. 1252, pp. 345–348. Springer, Berlin (1997)
14. Mühlich, M., Aach, T.: Analysis of multiple orientations. IEEE Transactions on Image Processing **18**(7), 1424–1437 (Jul 2009)
15. Payot, E., Guillemaud, R., Trousset, Y., Preteux, F.: An adaptive and constrained model for 3D X-ray vascular reconstruction. In: Grangeat, P., Amans, J.L. (eds.) Three-Dimensional Image Reconstruction in Radiation and Nuclear Medicine, Computational Imaging and Vision, vol. 4, pp. 47–57. Springer, Dordrecht (1996)
16. Rao, A.R., Schunck, B.G.: Computing oriented texture fields. CVGIP: Graphical Models and Image Processing **53**(2), 157–185 (Mar 1991)
17. Scharr, H.: Diffusion-like reconstruction schemes from linear data models. In: Franke, K., Müller, K.R., Nickolay, B., Schäfer, R. (eds.) Pattern Recognition, Lecture Notes in Computer Science, vol. 4174, pp. 51–60. Springer, Berlin (2006)
18. Shepp, L.A., Logan, B.F.: The Fourier reconstruction of a head section. IEEE Transactions on Nuclear Science **21**(3), 21–43 (Jun 1974)
19. Steidl, G., Teuber, T.: Anisotropic smoothing using double orientations. In: X. C. Tai, K. Mörken, M.L., Lie, K.A. (eds.) Scale Space and Variational Methods in Computer Vision. Lecture Notes in Computer Science, vol. 5567, pp. 477–489. Springer, Berlin (2009)
20. Weickert, J.: Coherence-enhancing diffusion filtering. International Journal of Computer Vision **31**(2/3), 111–127 (Apr 1999)
21. Weickert, J., ter Haar Romeny, B.M., Lopez, A., van Enk, W.J.: Orientation analysis by coherence-enhancing diffusion. In: Proc. 1997 Real World Computing Symposium. pp. 96–103. Tokyo, Japan (Jan 1997)
22. Williams, L.R., Jacobs, D.W.: Stochastic completion fields: A neural model of illusory contour shape and salience. Neural Computation **9**(4), 837–858 (May 1997)